

Photoinduced Electron Transfer between Cytochrome *c* Peroxidase (D37K) and Zn-Substituted Cytochrome *c*: Probing the Two-Domain Binding and Reactivity of the Peroxidase

Jian S. Zhou,[†] Suong T. Tran,[‡] George McLendon,^{*,‡} and Brian M. Hoffman^{*,†}

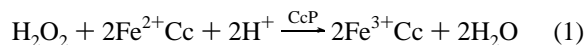
Contribution from the Departments of Chemistry, Northwestern University, Evanston, Illinois 60208-3113, and Princeton University, Princeton, New Jersey 08544

Received July 12, 1996[⊗]

Abstract: Cytochrome *c* peroxidase (CcP) binds cytochrome *c* (Cc) at two distinct surface binding domains, one having high affinity for Cc and the other having low affinity. The identity of the surface binding domains on CcP has been probed by studying photoinduced interprotein heme–heme electron transfer (ET) between Zn-substituted horse Cc, ZnCc, and a cloned cytochrome *c* peroxidase, CcP(D37K). Charge-reversal substitution of the negatively-charged residue Asp 37 of CcP by a positively-charged residue lysine greatly decreases the stoichiometric constant for 1:1 binding of Cc, from $8.5 \times 10^5 \text{ M}^{-1}$ for the wild-type CcP to $1.2 \times 10^4 \text{ M}^{-1}$ for CcP(D37K) ($\mu = 18 \text{ mM}$), thereby identifying residue 37 as part of the high-affinity binding domain of CcP(WT) (domain 1). This assignment is consistent with domain 1 as being that observed in a crystal of the Cc–CcP complex. The diminished ability of CcP(D37K) to bind Cc at domain 1 also suppresses binding of a second Cc molecule to form a ternary complex. However, the mutation sharply increases the reactivity of CcP: the stoichiometric rate constant for heme–heme ET within the 1:1 $^3\text{ZnCc–Fe}^{3+}\text{CcP(D37K)}$ complex is 4000 s^{-1} , much higher than that (40 s^{-1}) for $\text{ZnCc(H)–Fe}^{3+}\text{CcP(WT)}$. These results are explained by two-domain binding, where the high-affinity domain 1 has low heme–heme ET reactivity, while domain 2 has high heme–heme ET reactivity. The CcP(D37K) mutant exhibits greater reactivity than CcP(WT) because the mutational weakening of Cc-binding at CcP domain 1 increases the fraction of 1:1 complex where Cc is bound at the heme-reactive domain 2. Upon changing the ionic strength from 18 to 59 mN, the stoichiometric ET rate constant increases for the Cc–CcP(WT) complex, whereas it decreases 4-fold for the Cc(H)–CcP(D37K) complex, which indicates that the two distinct binding domains on CcP are differentially affected by ionic strength. This overall picture of ET between these two proteins is supported by a careful reconsideration of the most recent work from other laboratories. We hypothesize that domain 1 may make the dominant contribution to the direct reduction of the Trp 191 radical, while domain 2 provides the dominant kinetic site for ferryl–heme reduction.

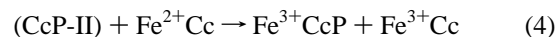
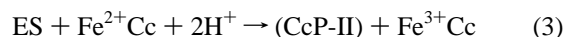
Introduction

In vivo, cytochrome *c* peroxidase (CcP) catalyzes the two-electron reduction of H_2O_2 by two molecules of Fe^{2+}Cc as the specific electron source (eq 1).^{1–3} In the first step of the CcP



catalytic cycle, the ferriheme resting state of CcP undergoes a two-electron oxidation by H_2O_2 (eq 2), producing the first stable species, compound ES. In this high-valence intermediate ES, one oxidizing equivalent is stored at the heme as a ferryl iron–oxo [$\text{Fe}^{\text{IV}}=\text{O}$]²⁺ species and the other as an amino acid radical on Trp 191.^{4–6} To complete the catalytic cycle, ES is one-equivalent reduced by Fe^{2+}Cc to form CcP-II (eq 3) which is

then reduced by a second molecule of Fe^{2+}Cc to the resting state (eq 4). The first reduction can occur *either* at the heme



or at the Trp radical, and thus CcP-II exists in two electronic configurations that are one-equivalent oxidized relative to the ferriheme resting state, one with an oxidized heme, CcP-II(h), and one with an oxidized Trp, CcP-II(r).^{7–9} These two forms exhibit a pH-dependent equilibrium,⁹ and the oxidizing equivalent can transfer between the two redox sites through an intramolecular electron-transfer (ET) process that is not fully understood and can be surprisingly slow.^{7,8,10} Because this catalytic cycle involves two Cc molecules and two spatially and electronically distinct redox centers of CcP, a key question is whether the two reductions occur by sequential reactions at a single binding domain on the CcP surface or whether there might

(7) Ho, P. S.; Hoffman, B. M.; Solomon, N.; Kang, C. H.; Margoliash, E. *Biochemistry* **1984**, *23*, 4122–4128.

(8) Ho, P. S.; Hoffman, B. M.; Kang, C. H.; Margoliash, E. *J. Biol. Chem.* **1983**, *258*, 4356–4363.

(9) Coulson, A. F. W.; Erman, J. E.; Yonetani, T. *J. Biol. Chem.* **1971**, *246*, 917–924.

(10) Summers, F. E.; Erman, J. E. *J. Biol. Chem.* **1988**, *263*, 14267–14275.

[†] Northwestern University.

[‡] Princeton University.

[⊗] Abstract published in *Advance ACS Abstracts*, December 1, 1996.

(1) Bosshard, H. R.; Anni, H.; Yonetani, T. In *Peroxidases in Chemistry and Biology, Vol. II*; Everse, J., Everse, K. E., Grisham, M. B., Eds.; CRC Press: Boca Raton, FL, 1991; pp 51–84.

(2) Dawson, J. H. *Science* **1988**, *240*, 433–439.

(3) Yonetani, T. In *The Enzymes, Vol XIII*; Boyer, P. D., Ed.; Academic Press: Orlando, FL, 1976; pp 345–361.

(4) Sivaraja, M.; Goodin, D. B.; Smith, M.; Hoffman, B. M. *Science* **1989**, *245*, 738–740.

(5) Houseman, A. L. P.; Doan, P. E.; Goodin, D. B.; Hoffman, B. M. *Biochemistry* **1993**, *32*, 4430–4443.

(6) Huyett, J. E.; Doan, P. E.; Gurbel, R.; Houseman, A. L. P.; Sivaraja, M.; Goodin, D. B.; Hoffman, B. M. *J. Am. Chem. Soc.* **1995**, *117*, 9033–9041.

be two ET-active domains, opening the possibility that there are even different "pathways"^{11–14} for heme and Trp reductions.

Extensive studies have been undertaken to address this key question.^{11,15–40} In particular, it is possible to examine heme–heme ET within the Cc–CcP complex by monitoring the ET cycle comprised of (i) photoinduced ET from a Zn(II)-substituted protein, ZnCcP or ZnCc, to the corresponding partner, Fe³⁺Cc or Fe³⁺CcP, followed by (ii) the return of the resulting charge-transfer intermediate, [(ZnCcP)⁺,Fe²⁺Cc] or [(ZnCc)⁺,Fe²⁺CcP], to the ground state.^{11,15} The present studies employ ZnCc. Photoinduced ET from ZnCc to the ferri-heme of resting state CcP is an excellent model for the reduction of the heme site in compound ES and in the heme-oxidized CcP-II(h) because ZnCc is a structurally and electrostatically faithful analog of the corresponding ferrous protein, as shown by solution NMR studies.^{41,42} As a result, the two forms of Cc should bind similarly to CcP and transfer electrons along the same pathways;¹¹ secondarily, the reactions have comparable driving forces.^{15,43} A key virtue of using Zn-substituted proteins to study heme–heme ET between CcP and Cc is that they

simplify the complicated problem presented by the presence of the two redox-active centers in CcP and of the two interconverting forms of CcP-II. By eliminating the oxidized Trp as a possible participant in reactions, one isolates and can cleanly address questions of binding and interfacial dynamics. Once these are understood, one can characterize the heme–heme ET event itself, all without complication from the involvement of the Trp radical and of interconversion between the two forms of CcP-II. The processes that involve the Trp then can be addressed by reaction ZnCc with ES itself or by the complementary technique of surface redox modification, and the results can be embedded in the overall picture of binding, docking, and heme–heme reactivity.

Kinetic measurements^{18–21} showed that CcP can bind two Cc molecules simultaneously to form a ternary complex, as first proposed by Kang et al. in the 1970s.⁴⁴ This finding about the 2:1 stoichiometry of the Cc–CcP complex has been confirmed by other techniques, including potentiometric titrations,⁴⁵ stopped-flow,^{29,30} energy transfer,^{46,47} cross-linking studies of binding between FeCc and FeCcP systems,⁴⁸ and electrostatics calculations.^{49–52} All these studies refuted the earlier belief that only 1:1 binding occurred and, more importantly, confirmed that CcP has two distinct binding domain. Using a redox-inert inhibitor,²¹ we definitively demonstrated that one Cc molecule binds tightly at a surface domain of CcP having low heme ET reactivity, whereas the second Cc molecule binds weakly at a second distinct domain having markedly greater (~10³) reactivity. Because of the existence of two possible binding domains (or ET-active domains) on CcP, Cc and CcP form a system that is extremely useful for determining the factors that control biological electron transfer, such as interfacial dynamics, recognition, and ET pathways.

Although the kinetic studies with the wild-type yeast CcP (CcP(WT)) demonstrate the presence of two binding domains on CcP, they do not provide any information about the location of these domains. This question can be approached by site-directed mutagenesis techniques. Poulos and Kraut⁵³ generated a computer graphic model for a 1:1 Cc–CcP complex on the basis of optimization of the electrostatic interactions between complementary charged groups. In this computer model,⁵³ Asp 37 of CcP and Lys 13 of Cc are one pair of charge groups among many specific ionic interactions. The predicted Poulos–Kraut binding site of CcP for Cc is different from, but overlaps with, a binding site identified in a crystal of 1:1 complex where Asp 37 is near the center of the interaction surface.⁵⁴ To relate these structural models with function, the negatively-charged residue Asp 37 of CcP was mutated to a positively-charged lysine to probe the nature of the ionic interactions in the Cc–CcP complex.^{24,25} This mutation of Asp 37 to Lys 37 causes more than a 10-fold decrease in binding affinity for Cc(H) and

(11) Nocek, J. M.; Zhou, J. S.; DeForest, S.; Priyadarshy, S.; Beratan, D. N.; Onuchic, J. N.; Hoffman, B. M. *Chem. Rev.* **1996**, *96*, 2459–2489.

(12) Winkler, J. R.; Gray, H. B. *Chem. Rev.* **1992**, *92*, 369–379.

(13) Priyadarshy, S.; Skourtis, S. S.; Risser, S. M.; Beratan, D. N. *J. Chem. Phys.* in press.

(14) Beratan, D. N.; Onuchic, J. N.; Winkler, J. R.; Gray, H. B. *Science* **1992**, *258*, 1740–1741.

(15) Hoffman, B. M.; Natan, M. J.; Nocek, J. M.; Wallin, S. A. *Struct. Bonding* **1991**, *75*, 85–108.

(16) Wallin, S. A.; Stemp, E. D. A.; Everest, A. M.; Nocek, J. M.; Netzel, T. L.; Hoffman, B. M. *J. Am. Chem. Soc.* **1991**, *113*, 1842–1844.

(17) Everest, A. M.; Wallin, S. A.; Stemp, E. D. A.; Nocek, J. M.; Mauk, A. G.; Hoffman, B. M. *J. Am. Chem. Soc.* **1991**, *113*, 4337–4338.

(18) Stemp, E. D. A.; Hoffman, B. M. *Biochemistry* **1993**, *32*, 10848–10865.

(19) Zhou, J. S.; Hoffman, B. M. *J. Am. Chem. Soc.* **1993**, *115*, 11008–11009.

(20) Zhou, J. S.; Hoffman, B. M. *Science* **1994**, *265*, 1693–1696.

(21) Zhou, J. S.; Nocek, J. M.; DeVan, M. L.; Hoffman, B. M. *Science* **1995**, *269*, 204–207.

(22) McLendon, G.; Hake, R. *Chem. Rev.* **1992**, *92*, 481–490.

(23) Hake, R.; McLendon, G.; Corin, A.; Holzschu, D. *J. Am. Chem. Soc.* **1992**, *114*, 5442–5443.

(24) Corin, A. F.; Hake, R. A.; McLendon, G.; Hazzard, J. T.; Tollin, G. *Biochemistry* **1993**, *32*, 2756–2762.

(25) Corin, A. F.; McLendon, G.; Zhang, Q.; Hake, R. A.; Falvo, J.; Lu, K. S.; Ciccarelli, R. B.; Holzschu, D. *Biochemistry* **1991**, *30*, 11585–11595.

(26) Pappa, H. S.; Poulos, T. L. *Biochemistry* **1995**, *34*, 6573–6580.

(27) Pappa, H. S.; Tajbaksh, S.; Saunders, A. J.; Pielak, G. J.; Poulos, T. L. *Biochemistry* **1996**, *35*, 4837–4845.

(28) Erman, J. E.; Vitello, L. B.; Mauro, J. M.; Kraut, J. *Biochemistry* **1989**, *28*, 7992–7995.

(29) Matthis, A. L.; Erman, J. E. *Biochemistry* **1995**, *34*, 9985–9990.

(30) Matthis, A. L.; Vitello, L. B.; Erman, J. E. *Biochemistry* **1995**, *34*, 9991.

(31) Ferrer, J. C.; Turano, P.; Banci, L.; Bertini, I.; Morris, I. K.; Smith, K. M.; Smith, M.; Mauk, A. G. *Biochemistry* **1994**, *33*, 7819–7829.

(32) Geren, L.; Hahm, S.; Durham, B.; Millett, F. *Biochemistry* **1991**, *30*, 9450–9457.

(33) Hahm, S.; Durham, B.; Millett, F. *Biochemistry* **1992**, *31*, 3472–3477.

(34) Miller, M. A.; Geren, L.; Han, G. W.; Saunders, A.; Beasley, J.; Pielak, G. J.; Durham, B.; Millett, F.; Kraut, J. *Biochemistry* **1996**, *35*, 667–673.

(35) Hahm, S.; Miller, M. A.; Geren, L.; Kraut, J.; Durham, B.; Millett, F. *Biochemistry* **1994**, *33*, 1473–1480.

(36) Liu, R.; Miller, M. A.; Han, G. W.; Hahm, S.; Geren, L.; Hibdon, S.; Kraut, J.; Durham, B.; Millett, F. *Biochemistry* **1994**, *33*, 8678–8685.

(37) Miller, M. A.; Vitello, L.; Erman, J. E. *Biochemistry* **1995**, *34*, 12048–12058.

(38) Miller, M. A.; Liu, R.; Hahm, S.; Geren, L.; Hibdon, S.; Kraut, J.; Durham, B.; Millett, F. *Biochemistry* **1994**, *33*, 8686–8693.

(39) Miller, M. A.; Hazzard, J. T.; Mauro, J. M.; Edwards, S. L.; Simons, P. C.; Tollin, G.; Kraut, J. *Biochemistry* **1988**, *27*, 9081–9088.

(40) Miller, M. A.; Bandyopadhyay, D.; Mauro, J. M.; Traylor, T. G.; Kraut, J. *Biochemistry* **1992**, *31*, 2789–2797.

(41) Moore, G. R.; Williams, R. J. P.; Chien, J. C. W.; Dickinson, L. C. *J. Inorg. Biochemistry* **1980**, *12*, 1–15.

(42) Anni, H.; Vanderkooi, J. M.; Mayne, L. *Biochemistry* **1995**, *34*, 5744–5753.

(43) Fossett, M. E.; Nocek, J. M.; Ellis, W. R. J.; Hoffman, B. M. *J. Am. Chem. Soc.* submitted.

(44) Kang, C. H.; Ferguson-Miller, S.; Margoliash, E. *J. Biol. Chem.* **1977**, *252*, 919–926.

(45) Mauk, M. R.; Ferrer, J. C.; Mauk, A. G. *Biochemistry* **1994**, *33*, 12609–12614.

(46) Kornblatt, J. A.; English, A. M. *Eur. J. Biochemistry* **1986**, *155*, 505–511.

(47) Suong, T. T.; Nocek, J. M.; Hoffman, B. M.; McClendon, G. L. Manuscript in preparation.

(48) Moench, S. J.; Satterlee, J. D.; Erman, J. E. *Biochemistry* **1987**, *26*, 3821–3826.

(49) Northrup, S. H.; Boles, J. O.; Reynolds, J. C. L. *Science* **1988**, *241*, 67–70.

(50) Northrup, S. H.; Boles, J. O.; Reynolds, J. C. L. *J. Phys. Chem.* **1987**, *91*, 5991–5998.

(51) Northrup, S. H.; Thomasson, K. A. *FASEB J.* **1992**, *6*, A474.

(52) Northrup, S. H.; Reynolds, J. C. L.; Miller, C. M.; Forrest, K. J.; Boles, J. O. *J. Am. Chem. Soc.* **1986**, *108*, 8162–8170.

(53) Poulos, T. L.; Kraut, J. *J. Biol. Chem.* **1980**, *255*, 10322–10330.

(54) Pelletier, H.; Kraut, J. *Science* **1992**, *258*, 1748–1755.

changed the steady-state kinetics from biphasic for CcP(WT) to monophasic for CcP(D37K).²⁵ These results indicated that, even though Asp 37 of CcP does not form a direct salt bridge with Cc(H) in the form of the complex observed in the crystal structure⁵⁴ of the 1:1 Cc(H)–CcP complex, it certainly is included in the functionally important strong binding domain (domain 1).

In this paper, we report a detailed kinetic study of the ET photocycle involving ZnCc and the CcP(D37K) mutant, thereby combining for the first time this kinetic approach with the use of an affinity mutant to probe multidomain binding and reactivity. We confirm that the mutation of Asp 37 to Lys 37 lowers the affinity for binding one Cc molecule by more than 10-fold at pH 7, and thus that this residue is included in the strong binding domain on CcP. However, while the affinity is lowered, the rate constant for the heme–heme electron transfer from ³ZnCc to Fe³⁺CcP(D37K) within the 1:1 stoichiometric complex is *much* higher (~10³) than that for wild-type yeast Fe³⁺CcP. Such results indicate that Cc bound at the (unidentified) weak binding domain of CcP is much more reactive for heme–heme electron transfer than is Cc bound at the strong binding (Asp 37) domain. The influence of the mutation in weakening Cc-binding at domain 1 on CcP increases the *fraction* of the form of the 1:1 complex where Cc is bound at the heme-reactive domain 2, thereby causing CcP(D37K) mutant to exhibit greater reactivity than CcP(WT). The analysis that underlies these conclusions further is used to correct recent claims³⁴ that Cc binds at only one domain on the CcP surface.

Experimental Section

Materials. Monobasic and dibasic potassium phosphate and potassium chloride were obtained from Fisher Co. Distilled water was purified by a Millipore Milli-Q water purification system. Sephadex G25 and horse heart cytochrome *c*, type VI, were purchased from Sigma Chemical Co.

Zinc cytochrome *c* (ZnCc) was prepared from horse heart cytochrome *c* according to the published procedure.⁵⁵ ZnCc was purified by cation-exchange chromatography on a column of CM-52 sized at 2.5 cm × 40 cm. The column was equilibrated with a 10 mM potassium phosphate buffer at pH 7.0; an 85 mM potassium phosphate buffer at pH 7.0 was the eluent. The major band (second band) was used in further experiments. The procedures for the preparation and purification of CcP(D37K) were published previously.^{24,25}

Methods. The ET kinetics were performed by laser flash kinetic spectrophotometry¹⁸ with the 532-nm output of a Q-switched Nd:YAG laser under anaerobic conditions at pH 7.0 and 20° ± 0.2 °C. The transient digitizer (LeCroy 9310L) collects 50 000 data points in a single kinetic trace; before analysis, this was compressed logarithmically to 3000 data points. The decays of the triplet excited state of ZnCc, ³ZnCc, were monitored at 460 nm, where the difference in absorbance between ³ZnCc and ZnCc is near the maximum. Each trace was an average of 10 shots. The formation and decay of the resulting charge-transfer intermediate, [(ZnCc)⁺, Fe²⁺CcP(D37K)], were monitored at a wavelength of 435 nm, the isosbestic point for the ³ZnCc–ZnCc absorbance. Data collection for slow processes involves baseline “live subtraction”, i.e., alternate collection of data and baseline (without laser pulse) traces, subtracting the former from the latter to correct for any baseline instability on a long time scale. At least 50 shots were collected and averaged to enhance the signal-to-noise ratio. The kinetics of the ET between ³ZnCc and Fe³⁺CcP(D37K) was studied by using the method of Stern–Volmer reverse titration developed recently,²⁰ in which the quencher, Fe³⁺CcP(D37K), was held at a fixed concentration while being titrated with the photoexcitable probe molecule, ZnCc. The laser power was controlled with a tunable polarizing beam splitter.

If ZnCc and the Fe³⁺CcP(D37K) mutant bind in a 1:1 *stoichiometry* (independent of whether this binding involves multiple binding

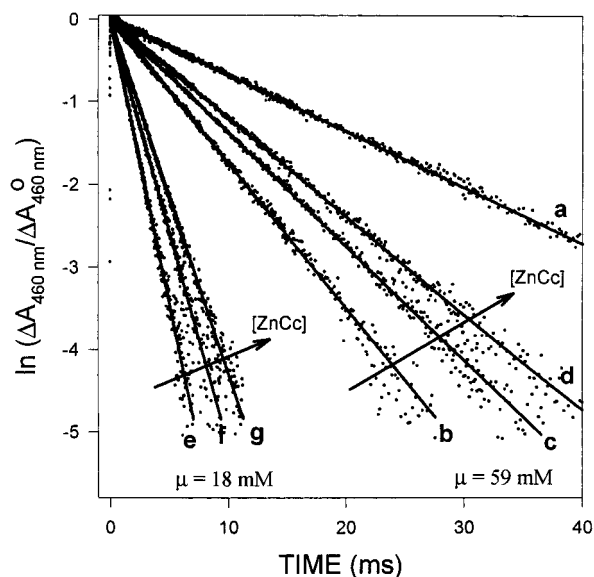


Figure 1. Semilog plots of the typical decay traces of the triplet excited state of ZnCc in phosphate buffers (pH 7.0) and at 20 °C. Trace a: [ZnCc] = 10 μM, [Fe³⁺CcP(D37K)] = 0 at μ = 18 mM. Traces b–d: [Fe³⁺CcP(D37K)] = 13.6 μM, [ZnCc] = 1.0, 51.4, and 103.8 μM, respectively, at μ = 59 mM. Traces e–g: [Fe³⁺CcP(D37K)] = 16.2 μM, [ZnCc] = 4.5, 43.4, and 94.6 μM, respectively, at μ = 18 mM.

domains), the fraction of the bound ZnCc over the total ZnCc concentration, f_1 , is given by eq 5, where [ZnCc]₀ and

$$f_1 = \frac{[\text{ZnCc}, \text{Fe}^{3+} \text{CcP(D37K)}]}{[\text{ZnCc}]_0} = \frac{([\text{ZnCc}]_0 + [\text{Fe}^{3+} \text{CcP(D37K)}]_0 + 1/K_A)/2[\text{ZnCc}]_0 - \{([\text{ZnCc}]_0 + [\text{Fe}^{3+} \text{CcP(D37K)}]_0 + 1/k_A)^2 - 4[\text{ZnCc}]_0[\text{Fe}^{3+} \text{CcP(D37K)}]_0\}^{1/2}/2[\text{ZnCc}]_0}{([\text{ZnCc}]_0 + [\text{Fe}^{3+} \text{CcP(D37K)}]_0 + 1/K_A)/2[\text{ZnCc}]_0 - \{([\text{ZnCc}]_0 + [\text{Fe}^{3+} \text{CcP(D37K)}]_0 + 1/k_A)^2 - 4[\text{ZnCc}]_0[\text{Fe}^{3+} \text{CcP(D37K)}]_0\}^{1/2}/2[\text{ZnCc}]_0} \quad (5)$$

[Fe³⁺CcP(D37K)]₀ are the total concentrations of the respective proteins and [ZnCc, Fe³⁺CcP(D37K)] is the total concentration of the complex.

The kinetic traces for the ET intermediate collected for 0 ≤ *t* ≤ 10 ms have been analyzed according to eq 6, as discussed in the Results section. Here, ΔA₀ = Δε[³ZnCc]₀k_{obs}, where Δε, [³ZnCc]₀, and k_{obs}

$$\Delta A_{435}(t) = \frac{\Delta A_0}{k_{\text{rise}} - k_{\text{fall}}} (e^{-k_{\text{fall}}t} - e^{-k_{\text{rise}}t}) + \frac{\Delta A_\infty}{k_{\text{rise}} - k_{\text{fall}}} [k_{\text{rise}}(1 - e^{-k_{\text{obs}}t}) + k_{\text{fall}}(e^{-k_{\text{rise}}t} - 1)] \quad (6)$$

are the difference in extinction coefficient between intermediate and ground state, the total concentration of ³ZnCc, and the rate constant of ³ZnCc decay, respectively; the residual absorbance is ΔA_∞ ∝ Δε[k_{off}/(k_{off} + k_b)]; k_{rise} and k_{fall} are the rate constants respectively for the growth and decay of ΔA₄₃₅.

Results

Quenching of the ³ZnCc by Fe³⁺CcP(D37K). The photo-induced electron transfer from ³ZnCc to Fe³⁺CcP is studied by examining quenching of the ³ZnCc as monitored at 460 nm. In the absence of Fe³⁺CcP(D37K), the decay of ³ZnCc is exponential (trace a in Figure 1). The intrinsic rate constant of k_D = 67 ± 3 s⁻¹ is independent of ionic strength from 18 to 59 mM and of the ZnCc concentration from 1 to 105 μM. When Fe³⁺CcP(D37K) is present in the solution, the ³ZnCc decay remains exponential but is accelerated. During a reverse titration in which ZnCc is progressively added into a solution of Fe³⁺CcP at a fixed concentration, the decay constant depends on the ionic strength and the concentration of ZnCc (traces b–g in Figure 1). The quenching constants (k_q = k_{obs} - k_D) are plotted in Figure 2 for titrations at 18 and 59 mM ionic strengths. The

(55) Vanderkooi, J. M.; Adar, F.; Erecinska, M. *Eur. J. Biochemistry* 1976, 64, 381–387.

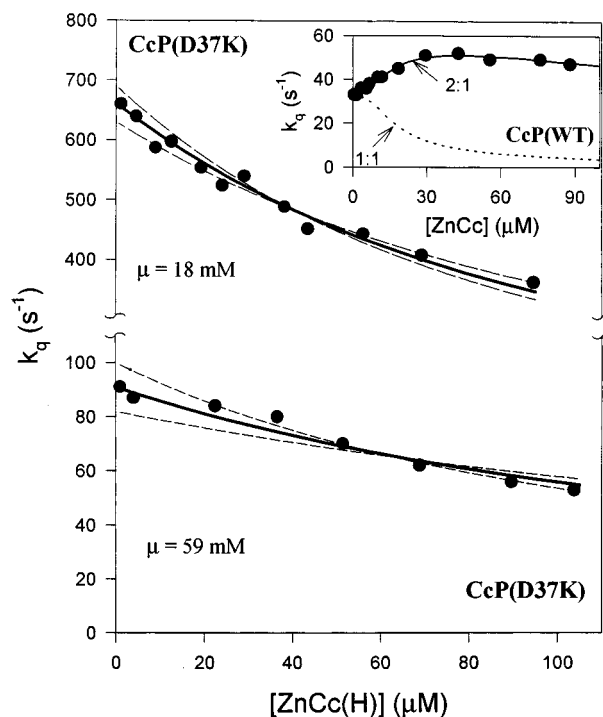


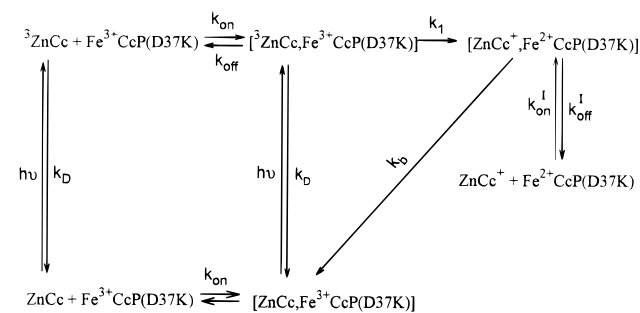
Figure 2. ET quenching rate of $^3\text{ZnCc}$ by $\text{Fe}^{3+}\text{CcP(D37K)}$ as function of $[\text{ZnCc}]$ in phosphate buffer (pH 7.0) at 20°C . The solid lines are the theoretical fits to a 1:1 binding isotherm (eq 7) with $K_A = 7.3 \times 10^3 \text{ M}^{-1}$ (bottom) and $K_A = 1.26 \times 10^4 \text{ M}^{-1}$ (top). The dotted lines are the theoretical fits to eq 7, assuming the intercept values k_q^0 (eq 8) having a error of $\pm 5\%$ (top) and $\pm 10\%$ (bottom), respectively. Conditions: $[\text{Fe}^{3+}\text{CcP(D37K)}] = 16.2 \mu\text{M}$ at $\mu = 18 \text{ mM}$ (top) and $[\text{Fe}^{3+}\text{CcP(D37K)}] = 13.6 \mu\text{M}$ at $\mu = 59 \text{ mM}$ (bottom). Inset: ET quenching of $^3\text{ZnCc}$ by wild-type Fe^{3+}CcP as function of $[\text{ZnCc}]$ in phosphate buffer (pH 7.0 and $\mu = 18 \text{ mM}$) at 20°C . $[\text{Fe}^{3+}\text{CcP}] = 10.4 \mu\text{M}$. The solid line is the theoretical curve of a 2:1 binding model.²⁰ The dotted line is the theoretical prediction of a 1:1 binding model ($K_1 = 8.5 \times 10^5 \text{ M}^{-1}$ and $k_1 = 39 \text{ s}^{-1}$). The difference between the two curves, rather than the weak maximum in the experiment, confirms 2:1 binding.

quenching constants in both titrations are greatest at the lowest concentration of ZnCc and decrease monotonically. At $\mu = 18 \text{ mM}$, the quenching decreases from $k_q^0 \approx 670 \text{ s}^{-1}$ as $[\text{ZnCc}] \rightarrow 0$ to $k_q \approx 400 \text{ s}^{-1}$ at $[\text{ZnCc}] = 95 \mu\text{M}$; at $\mu = 59 \text{ mM}$, the quenching is diminished, and the quenching decreases from $k_q^0 \approx 90 \text{ s}^{-1}$ to $k_q \approx 60 \text{ s}^{-1}$ over the same ZnCc concentration range. This behavior contrasts sharply with that for wild-type cytochrome *c* peroxidase. A reverse titration of CcP(WT) at 18 mM ionic strength²⁰ begins with a very low value of the quenching constant as $[\text{ZnCc}] \rightarrow 0$, $k_q^0 \approx 35 \text{ s}^{-1}$. Rather than decreasing sharply and monotonically, as is required¹¹ for such a titration when binding has a 1:1 stoichiometry (Figure 2, inset), the quenching actually *increases* slightly to $k_q \approx 55 \text{ s}^{-1}$ at $[\text{ZnCc}] \approx 30 \mu\text{M}$ and then decreases slightly to $k_q \approx 50 \text{ s}^{-1}$ at the highest concentration employed.

At no point during a titration of $\text{Fe}^{3+}\text{CcP(D37K)}$ by ZnCc does an increase in the laser power from 1 to 80 mJ/pulse introduce a rapidly decaying component (on the microsecond timescale) or cause the decay of $^3\text{ZnCc}$ to become nonexponential, nor does it change the decay rate constant. The absorbance difference ($\Delta A_{460\text{nm}}$), created by photolysis of the solution, of $^3\text{ZnCc}$ at either ionic strength also is not significantly diminished by the presence of $\text{Fe}^{3+}\text{CcP(D37K)}$.

As we now describe, these observations together establish that, under the conditions of these experiments, there is no fast "static" quenching of $^3\text{ZnCc}$ by $\text{Fe}^{3+}\text{CcP(D37K)}$ within a preformed complex, and that the quenching kinetics can be treated by expressions appropriate for the rapid exchange limit,

Scheme 1



where the intracomplex electron transfer from $^3\text{ZnCc}$ to $\text{Fe}^{3+}\text{CcP(D37K)}$ is much slower than the association and dissociation of the complex. Scheme 1 depicts various processes for the $\text{ZnCc}-\text{Fe}^{3+}\text{CcP(D37K)}$ system in the solution. Irradiation of the solution with a laser produces the singlet excited state (not shown) of ZnCc , which rapidly undergoes intersystem crossing to form the triplet excited state. Like ground-state ZnCc , the ZnCc excited state exists in two forms—free and associated with $\text{Fe}^{3+}\text{CcP(D37K)}$. Because of the presence of the forms prior to irradiation, the observed decay of $^3\text{ZnCc}$ can be biexponential or exponential, depending on whether or not the rate constant (k_1) for the intracomplex ET is much faster than the rate constant (k_{off}) for the dissociation of the complex.

When dissociation of the complex is slower than intracomplex ET ($k_1 \gg k_{\text{off}}$), the "static quenching" process within the preformed complex and the diffusive quenching process between the free reactants occur on different time scales. In this case, if there is a significant amount of the preformed complex (more than $\sim 5\%$) in the solution, the decay of $^3\text{ZnCc}$ will be biphasic: (i) rapidly decaying, component is related to the intracomplex ET within the preformed complex, and (ii) slow, component reflects ET between free $^3\text{ZnCc}$ and free $\text{Fe}^{3+}\text{CcP(D37K)}$. This prediction based on the slow exchange mechanism ($k_1 \gg k_{\text{off}}$) is inconsistent with the observation that the $^3\text{ZnCc}$ decay is exponential in the presence of $\text{Fe}^{3+}\text{CcP(D37K)}$. Alternatively, because of the limited time resolution of the instrument, fast ET within the preformed complex might be undetectable, leading to an *apparent* exponential decay of $^3\text{ZnCc}$ at 460 nm in the presence of $\text{Fe}^{3+}\text{CcP(D37K)}$. However, if this were so, then there would be a significant decrease in the absorbance of $^3\text{ZnCc}$ at the apparent time zero on the addition of $\text{Fe}^{3+}\text{CcP(D37K)}$. Instead, the absorbance of $^3\text{ZnCc}$ at 460 nm at time zero does not decrease significantly when the $\text{Fe}^{3+}\text{CcP(D37K)}$ is added into the ZnCc solution.

A slow exchange mechanism might also be operative, yet lead to exponential decay of $^3\text{ZnCc}$, if the population of the preformed complex is very low, because of weak binding between ZnCc and $\text{Fe}^{3+}\text{CcP(D37K)}$. In this case, the faster decay component would not be resolved. However, for weak binding in the slow exchange limit ($k_1 \gg k_{\text{off}}$), the bimolecular diffusion step (k_{on}) is the controlling step in the quenching of $^3\text{ZnCc}$. As a result, the $^3\text{ZnCc}$ would decay in a second-order process, or with a rate constant that depends on the $^3\text{ZnCc}$ concentration (or the laser power). The finding that, in the presence of $\text{Fe}^{3+}\text{CcP(D37K)}$, the $^3\text{ZnCc}$ decays with one rate constant, independent of the laser power (i.e., the $^3\text{ZnCc}$ concentration), eliminates this possibility. These experimental results thus establish that there is no ultrafast ET between $^3\text{ZnCc}$ and $\text{Fe}^{3+}\text{CcP(D37K)}$ within the preformed complex.

Binding. As discussed in detail earlier,²⁰ for a system that exhibits only 1:1 binding, k_q *must* decrease monotonically during a reverse titration of $\text{Fe}^{3+}\text{CcP(WT)}$ with ZnCc , and thus the appearance of a maximum in k_q during this titration at 18 mM

Table 1. ET Rate Constants and Binding Constants Obtained from the One-Parameter Fits of Data into Eqs 5 and 7

	μ (mM)	k_q^o (s ⁻¹)	K_1 (M ⁻¹)	k_1 (s ⁻¹)	K_2 (M ⁻¹)	k_2 (s ⁻¹)
CcP(WT) ^a	18	33	8.5×10^5	40	4300	1540
CcP(D37K) ^b	59	91 ± 9	$(7.30 \pm 3.3) \times 10^3$	1006 ± 300		
	18	661 ± 30	$(1.26 \pm 0.30) \times 10^4$	3899 ± 550		

^a The averaged value of constants obtained from the inverse and reverse titrations,^{19,20} except for k_q^o , which is taken from ref 20. ^b Calculated from k_q^o and K_A according to eq 8.

ionic strength,²⁰ illustrated in Figure 2 (inset), is unambiguous proof that Cc binds to wild-type peroxidase in a 2:1 stoichiometry under these conditions. In contrast, the monotonic decrease in k_q during the titration of Fe³⁺CcP(D37K) requires only the involvement of a 1:1 ZnCc–CcP(D37K) complex in the quenching process. In this case, the rapid exchange limit requires that $k_1 < k_{on}[Fe^{3+}CcP(D37K)]$ and $k_1 \ll k_{off}$ (Scheme 1). Because intracomplex ET within the complex is the controlling step in the quenching of ³ZnCc by Fe³⁺CcP(D37K), the dissociated ³ZnCc and Fe³⁺CcP(D37K) always are in equilibrium with the complex [³ZnCc,Fe³⁺CcP(D37K)], and the triplet excited state of ZnCc decays exponentially then, regardless of the ³ZnCc and Fe³⁺CcP(D37K) concentration and binding constant. The quenching rate constant (k_q) measured at any point in a titration is determined by the fraction of the bound ZnCc, f_1 (eq 5), and the intracomplex ET rate constant.

$$k_q = k_q \frac{[ZnCc, Fe^{3+}CcP(D37K)]}{[ZnCc]_0} = k_1 f_1 \quad (7)$$

Because the interactions between the protein surfaces are unlikely to be affected by optical excitation of the zinc porphyrin within cytochrome *c*, we take the equilibrium constants, K_A , to be identical for binding CcP to both the ground state and excited triplet states of ZnCc.

The titration data in Figure 2 can be fitted directly to eqs 5 and 7 to determine the binding constant (K_A) and intracomplex ET rate constant (k_1). However, as can clearly be seen in Figure 2, in a reverse titration, where the quencher is at a fixed concentration, denoted $[Fe^{3+}CcP(D37K)]_0$, and the sensitizer ZnCc is the titrant, the quenching rate constant has a well-defined, nonzero limit (intercept) as $[ZnCc]_0 \rightarrow 0$, denoted as k_q^o . From eqs 5 and 7 this intercept can be written

$$k_q^o = k_1 K_A \frac{[Fe^{3+}CcP(D37K)]_0}{1 + K_A [Fe^{3+}CcP(D37K)]_0} \quad (8)$$

The experimental value for k_q^o , then, can be used with the relation between K_A and k_1 given by eq 8 to eliminate one of the two parameters (k_1 and K_A) that describe a 1:1 titration curve. In short, a reverse titration provides an additional input, the nonzero k_q^o intercept, that is not provided by the “trivial” $k_q = 0$ intercept in a ‘normal’ titration of a photodonor by a quencher. This makes the reverse titration more reliable than the normal titration for determining the intracomplex ET rate constant and the weak binding constant that clearly characterize the complex with the CcP mutant (Figure 2). The binding constants and intracomplex ET constants obtained by using this procedure to fit to the data by eqs 5 and 7 are reported in Table 1. The spread in the titration curves, calculated using 5% and 10% uncertainties in the respective intercept, k_q^o , for the experiments at 18 and 59 mM ionic strengths, is illustrated in Figure 2 and shows that the actual uncertainties in the kinetic parameters must be less than these limits. The good agreement shown between the experimental titration curves and those calculated using these values (Figure 2) clearly indicates that the measurements at both

ionic strengths are well described by eqs 5 and 7 for a 1:1 binding *stoichiometry*.

The binding constant for CcP(D37K) is modest, $K_A \approx 10^4$ M⁻¹, and does not change greatly between $\mu = 18$ and 59 mM. This contrasts with the high affinity and the strong ionic strength dependence shown by CcP(WT) for binding the first Cc, where K_A changes from $\sim 10^7$ to $\sim 10^5$ M⁻¹ over a similar change in ionic strength. The finding that the D37K mutation reduces K_A by more than 10-fold is consistent with the earlier studies.²⁵ The rate constant for CcP(D37K) drops *ca.* 4-fold, from $k_1 = 4000$ to 1000 s⁻¹, as the ionic strength is increased from $\mu = 18$ to 59 mM. In contrast, for CcP(WT), the rate constant *increases* from $k_1 = 40$ to 200 s⁻¹ when the ionic strength increases from 18 to 118 mM. As discussed below, even though the results for CcP(D37K) reflect a 1:1 binding *stoichiometry*, the changes in behavior with ionic strength indicate that the binding and reaction occur at two (or more) separate binding *domains*.

Kinetics of the ET Intermediate. Thermal back electron transfer between Fe²⁺CcP(D37K) and the ZnCc cation radical, ZnCc⁺, subsequent to the photoinitiated ET has been followed by monitoring the absorption of the ET intermediate, [ZnCc⁺,Fe²⁺-CcP(D37K)], at 435 nm, the isosbestic point for the ³ZnCc–ZnCc absorbance. At 18 mM ionic strength, the signal rises to a maximum within ~ 1 ms and then falls to a plateau value of one-half to one-third the maximum within 5–10 ms (Figure 3); this residual absorbance then decays very slowly (Figure 3, inset). This behavior is reflective of Scheme 1 in a process where the behavior for $t \leq 10$ ms primarily reflects the buildup of the charge-transferred complex D⁺A⁻ and its decay through both ET recombination and dissociation of the complex. The long-time trace is a second-order process in which the dissociated ET products, ZnCc⁺ and Fe²⁺CcP(D37K), reassociate and return to the initial state. This kinetic behavior of the ET intermediate was observed over the ZnCc concentration range 8.9–38.1 μ M (Figure 4). The kinetic traces for the ET intermediate collected for $0 \leq t \leq 10$ ms have been analyzed in the simplifying and well-justified limit where the recombination of the dissociated ET products is unimportant on this time scale. This analysis is equivalent to setting $k_{on}^1 = 0$ in Scheme 1. This leads to the description of the time course for the absorbance difference, given by eq 6.

All kinetic traces are well described by eq 6, with $k_{rise} \gg k_{obs}$ and $k_{fall} \approx k_{obs}$. In this case, one assigns the measured rate constants to those of Scheme 1 as follows: $k_{rise} = k_b + k_{off}$; $k_{fall} = k_{obs} = k_D + k_q$. To obtain the most reliable values of k_{rise} , a final analysis of all data with eq 6 has been carried out by fixing $k_{fall} = k_{obs}$, which is most reliably determined from the ³ZnCc decay at 460 nm. The rate constant for the appearance of the transient is independent of the ZnCc concentration ($8.9 \leq [ZnCc] \leq 38.1$ μ M, $k_{rise} = 2150 \pm 130$ s⁻¹), much greater than the triplet decay rate constant. This confirms that ET occurs within the bound protein–protein complex. The ET intermediate, formed by ET quenching of ³ZnCc by Fe³⁺CcP, also has been observed for solutions of 59 mM ionic strength. However, in this case the signal at 435 nm

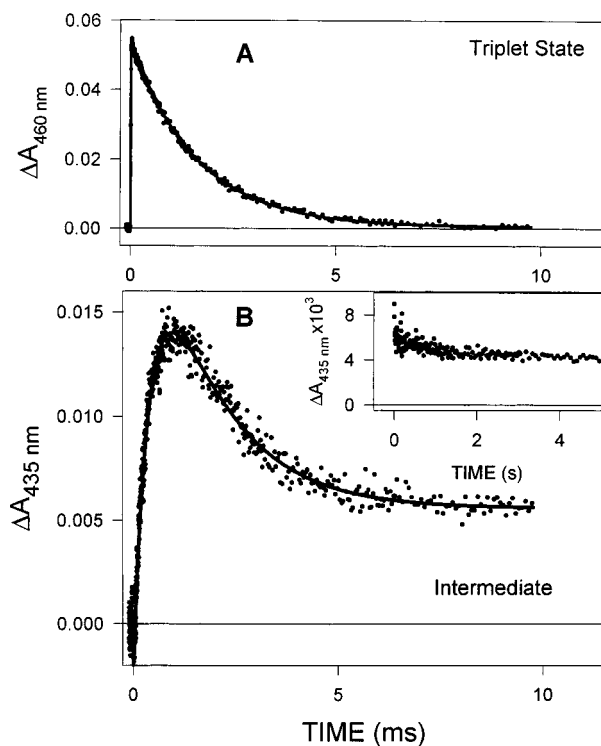


Figure 3. (A) The decay trace of ${}^3\text{ZnCc}$ at 460 nm. The solid line is the exponential fitting curve. (B) Kinetic progress curve for the ET intermediate monitored at 435 nm. The solid line is the theoretical fit obtained with a single rise-and-fall function (eq 6), using the following parameters: $k_r = 2286 \text{ s}^{-1}$, $k_f = k_{\text{obs}} = 665 \text{ s}^{-1}$, $\Delta A_{\infty} = 0.0057$, $\Delta A_0 = 0.0792$. Inset: Slow second-order decay of the residual change in absorbance (ΔA_{∞}) on a very long time scale. Conditions: $[\text{ZnCc}] = 12.5 \mu\text{M}$, $[\text{Fe}^{3+}\text{CcP(D37K)}] = 16.2 \mu\text{M}$ in phosphate buffer (pH 7.0) at $\mu = 18 \text{ mM}$ and $20 \text{ }^\circ\text{C}$.

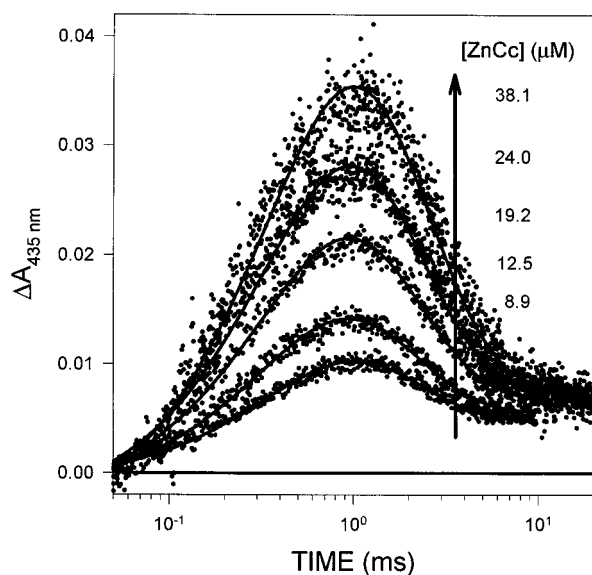


Figure 4. Kinetic progress curves for the ET intermediate monitored at 435 nm. Conditions: $[\text{Fe}^{3+}\text{CcP(D37K)}] = 16.2 \mu\text{M}$, $[\text{ZnCc}] = 8.9, 12.5, 19.2, 24.0,$ and $38.1 \mu\text{M}$, respectively (from bottom to top), in phosphate buffer (pH 7.0) at $\mu = 18 \text{ mM}$ and $20 \text{ }^\circ\text{C}$. The solid lines are the theoretical fits with eq 6.

from the intermediate is too small to be analyzed reliably,⁵⁶ and its kinetics were not investigated in further detail.

(56) Since at 59 mM ionic strength, almost 50% of the ZnCc triplet is not quenched by the $\text{Fe}^{3+}\text{CcP(D37K)}$, the kinetics of ET intermediate at this ionic strength is complicated by the intrinsic transient which is probably produced from the intraprotein ET between the Zn-porphyrin triplet and some residues inside ZnCc.

Analysis and Discussion

Previous work has shown that CcP(WT) can bind two Ccs simultaneously at two separate binding domains: one having high affinity and the other having low affinity.^{11,18–21,29,30,45,47–52} The complex with 2:1 stoichiometry has a *ca.* 10^3 -fold higher rate constant for direct heme–heme ET than does the 1:1 complex. It appears that this reflects an intrinsically higher reactivity at the weak binding domain, denoted domain 2. By use of the reverse titration protocol,²⁰ the difference between 1:1 and 2:1 binding can be accentuated, as shown in Figure 2 (inset), and this new experimental approach allowed us to confirm that the 2:1 stoichiometry is present even at high ionic strength, 118 mM.²⁰ The mutant CcP(D37K), obtained by a single charge-reversal on the CcP surface, behaves very differently from CcP(WT) in binding and heme–heme ET. Whereas a maximum in k_q is seen in the reverse titration of wild-type CcP by ZnCc,²⁰ k_q decreases monotonically in the reverse titration of $\text{Fe}^{3+}\text{CcP(D37K)}$ by ZnCc. The titration with the mutant is well-described by a 1:1 binding stoichiometry, even at the modest ionic strength of 18 mM, with an intermediate binding constant ($K_1 \approx 10^4 \text{ M}^{-1}$). This effect of the mutation on binding constant clearly substantiates the influence of residue 37 on the high-affinity binding domain. The weakened binding is accompanied by a sharply increased rate of ET, a decoupling of binding and reactivity that has been observed before. Moreover, the rate constant (k_1) for ET within the 1:1 complex shows a sharply different dependence on ionic strength for CcP(WT) and CcP(D37K): k_1 decreases for CcP(D37K) as the ionic strength increases, whereas it increases for CcP(WT) (Table 1).

Previous site-directed mutagenesis results were interpreted in terms of two “conformers” of a 1:1 adduct, corresponding to “exclusive” binding at two different sites within a single CcP binding domain.^{24,25} Given the observation of a 1:1 stoichiometry in the present study with CcP(D37K), our results, of course, could be interpreted similarly. However, the definitive demonstration that there are two distinct binding domains on CcP, as shown by the formation of the ternary complex, $[\text{Cc}_2\text{CcP}]$,^{11,18–21,29,30,45–52} indicates that the “conformers” are to be viewed as involving microscopically distinct binding domains that can be populated *nonexclusively*, and simultaneously in the case of CcP(WT) under appropriate conditions. As we now discuss, the results reported here indicate that the mutation of Asp 37 of CcP to Lys produces an *apparent* paradox: weakened binding at the poorly-reacting but tightly-binding domain, domain 1, has the effect of increasing the occupancy of the highly reactive domain 2, and this is the cause of the increase in the observed (stoichiometric) rate for ET in the 1:1 complex between the mutant CcP and Cc. We further show that measurements carried out by others through the use of ruthenium-labeled Cc^{32–36,38} strongly support the conclusion that the surface of CcP has two domains for binding Cc and that these have different reactivities for ET with the heme and Trp radical sites.

Stoichiometric vs Domain Constants. To begin, we recall that, in the case of multivalent binding, one must distinguish between stoichiometric (macroscopic) and domain or site (microscopic) equilibria. The meaning of these terms is illustrated in Figure 5. Experiments always yield stoichiometric binding constants; domain or site binding constants are experimentally inaccessible unless one monitors, say with NMR, the domains themselves. For an “enzyme” such as CcP that can simultaneously bind two “substrate” proteins, here Cc, at two distinct domains, the relations between the stoichiometric (macroscopic) and domain (microscopic) binding constants are

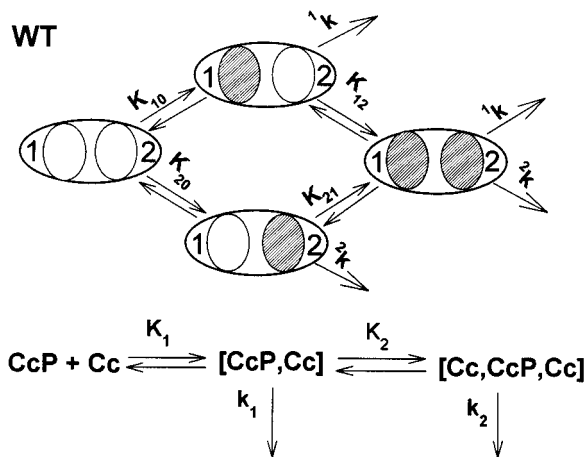


Figure 5. Schematic representation of domain (microscopic) and stoichiometric (macroscopic) bindings of Cc on CcP. The K_{10} and ${}^i k$ ($i = 1, 2$) are domain binding constants and domain ET rate constants, respectively. K_i and k_i ($i = 1, 2$) are stoichiometric binding and ET rate constants.

given by eqs 9–11.^{20,57–59} Here, K_{10} ($i = 1, 2$) is the domain

$$K_1 = K_{10} + K_{20} \quad (9)$$

$$K_2 = \frac{K_{10}K_{12}}{K_{10} + K_{20}} \quad (10)$$

$$K_1K_2 = K_{10}K_{12} = K_{20}K_{21} \quad (11)$$

binding constant for binding one Cc at domain i of free CcP; K_{i2} ($i = 1, 2$) is the domain binding constant for binding the second Cc to the 1:1 Cc:CcP complex, where the Cc is bound at domain i of CcP. CcP is not big enough to bind two Cc molecules without some interaction between them, and one must, therefore, expect that the domain constants will reflect this, with $K_{10} > K_{21}$ and $K_{20} > K_{12}$, because of the presence of repulsive interactions between the two bound Ccs in the ternary complex.

Likewise, when the complexes and the components are in rapid exchange, the stoichiometric (macroscopic) rate constants defined by Scheme 1 and measured by a titration experiment, in fact, are a composite of the domain (microscopic) constants associated with the two binding domains on CcP, as defined in Figure 5. The relations are as follows:

$$\begin{aligned} k_1 &= {}^1k \frac{K_{10}}{K_{10} + K_{20}} + {}^2k \frac{K_{20}}{K_{10} + K_{20}} = {}^1k f_1 + {}^2k f_2 \\ &= {}^1k + ({}^2k - {}^1k) \frac{K_{20}}{K_1} = {}^1k + ({}^2k - {}^1k) f_2 \end{aligned} \quad (12)$$

$$k_2 = {}^1k + {}^2k \quad (13)$$

In particular, the stoichiometric constant k_1 depends not only on the two microscopic single-domain rate constants, 1k and 2k , but also on the two microscopic binding constants, K_{10} and K_{20} , through the functions $f_i = K_{i0}/K_1$ ($i = 1, 2$). The ratios f_1 and f_2 describe the fraction of 1:1 complex in solution that has Cc bound respectively at domains 1 and 2 $\{i = 1; [1,0]$ and $[0,1]$ in Figure 5}.

(57) Klotz, I. M. *Introduction to Biomolecular Energetics, Including Ligand-Receptor Interactions*; Academic Press: New York, 1986.

(58) Van Holde, K. E. *Physical Biochemistry*, 2nd ed.; Prentice-Hall: Englewood Cliffs, NJ, 1985.

(59) Strickland, S.; Palmer, G.; Massey, V. *J. Biol. Chem.* **1975**, *250*, 4048–4052.

It can be seen clearly from eqs 9–11 that *both* of the experimentally-determined stoichiometric binding constants (K_1 and K_2) will change even if only one domain binding constant, e.g., K_{10} , changes for any reason. Likewise, the rate constant k_1 will change, whereas k_2 is independent of domain binding constants (eq 12). This has been often ignored in the design and conduct of experiments and in the interpretation of experimental results of binding stoichiometry and domains probed by site-directed mutagenesis techniques.

Effects of the Mutation on Domain Binding Constants and Binding Stoichiometry. With the consideration of eqs 5–9, it is straightforward to understand the observed effects of the mutation of Asp 37 to Lys 37 on CcP on binding stoichiometry and affinity. For CcP(WT)–Cc complexes, we have previously determined the stoichiometric binding constants at 18 mM ionic strength and pH 7.0: $K_1 = 8.5 \times 10^5 \text{ M}^{-1}$ and $K_2 = 4.3 \times 10^3 \text{ M}^{-1}$. Although the domain binding constants cannot be determined directly, it is possible to make reasonable estimates of the domain constants for this system at this ionic strength through use of eqs 9–11. Experiment shows that $K_{10} \gg K_{20}$ for CcP(WT), in which case $K_{10} \approx K_1 = 8.5 \times 10^5 \text{ M}^{-1}$, $K_{12} \approx K_2 = 4.3 \times 10^3 \text{ M}^{-1}$, $K_{20} > K_{12} = 4.3 \times 10^3 \text{ M}^{-1}$, and $K_{21} < K_{10} = 8.5 \times 10^5 \text{ M}^{-1}$ (Table 2).

For the CcP(D37K) mutant, substitution of the negatively-charged residue Asp 37 with a positively-charged lysine greatly weakens the Cc-binding affinity at domain 1 (K_{10}), because the mutation not only eliminates a negative charge on CcP but also introduces simultaneously a repulsive interaction between the positively charged Lys 37 of CcP(D37K) and the positively-charged lysine residues located at the heme-exposed edge (docking domain) of Cc. This is clearly shown by the sharp decrease in the stoichiometric binding constant K_1 from 10^6 to 10^4 M^{-1} . Considering that the residue 37 probably is more than 10 \AA away^{49,50} from the second binding domain of CcP, we may, to a first approximation, assume that the binding affinity at domain 2 (K_{20}) is not substantially affected by the mutation in CcP(D37K). With this assumption, we can use the thermodynamic cycle implicit in Figure 5 to make the following estimates for CcP(D37K): $K_1(\text{D37K}) = 1.26 \times 10^4 \text{ M}^{-1} > K_{20}(\text{D37K}) \geq K_2(\text{WT}) = 4.3 \times 10^3 \text{ M}^{-1}$ and $K_{10}(\text{D37K}) \leq 8.3 \times 10^3 \text{ M}^{-1}$ (Table 2).

Based on these considerations, it is easy to understand why $K_1(\text{D37K}) < K_1(\text{WT})$, yet $K_2(\text{WT}) > K_2(\text{D37K})$, with the latter having the consequence that a 2:1 ternary complex is observed for CcP(WT) but not the CcP(D37K) mutant. The concentration of ternary complex depends on the product, $K_1K_2 = K_{10}K_{12}$ (eq 11). Thus, even if K_{12} is unaffected by the mutation, according to eq 10 a major decrease in K_{10} for the mutant would make $K_2(\text{D37K}) \ll K_2(\text{WT}) \approx 4 \times 10^3 \text{ M}^{-1}$. Put another way, the formation of 2:1 Cc–CcP complex requires two consecutive binding steps: one of moderately weak strength, followed by an even weaker one. Thus, for the mutant, the amount of 2:1 complex should be negligibly small, so that only the complexes with 1:1 stoichiometries contribute to the quenching of ${}^3\text{ZnCc}$ by $\text{Fe}^{3+}\text{CcP}(\text{D37K})$ under our experimental conditions.

Domain Heme–Heme ET Rate Constants. Although the *stoichiometric* constants for binding of Cc are greatly lessened by the mutation of Asp 37 to Lys 37 in CcP, the *stoichiometric* intracomplex ET rate constant k_1 is greatly enhanced, with k_1 increasing from 40 s^{-1} ²⁰ for CcP(WT) to 3900 s^{-1} for CcP(D37K) (Table 1). This can be understood in terms of eq 12, which shows that, even for a 1:1 binding stoichiometry, the stoichiometric rate constant k_1 is a weighted average of the two domain rate constants, which are associated with the two conformers of the 1:1 complex. Analysis of the data in the inset to Figure 2 indicates that, even at the quenching maximum,

Table 2. Estimates of Domain Constants at pH 7.0, $\mu = 18$ mM, and 20 °C

	K_{10} (M ⁻¹)	K_{20} (M ⁻¹)	K_{12} (M ⁻¹)	K_{21} (M ⁻¹)	1k (s ⁻¹)	2k (s ⁻¹)
CcP(WT)	8.5×10^5	$>4.3 \times 10^3$	4.3×10^3	small ^a	$\leq 4.5^b$	$>2500^b$
CcP(D37K)	$\leq 8.3 \times 10^3$	$\geq 4.3 \times 10^3$	small ^c	small ^c	<i>d</i>	$>3900^e$

^a $K_{21} < K_{10}$ as described in the text. ^b References 19 and 20. ^c $K_{12} \ll 4.3 \times 10^3$ M⁻¹. ^d Undetermined. ^e By eq 12, $^2k > k_1$ (Table 1).

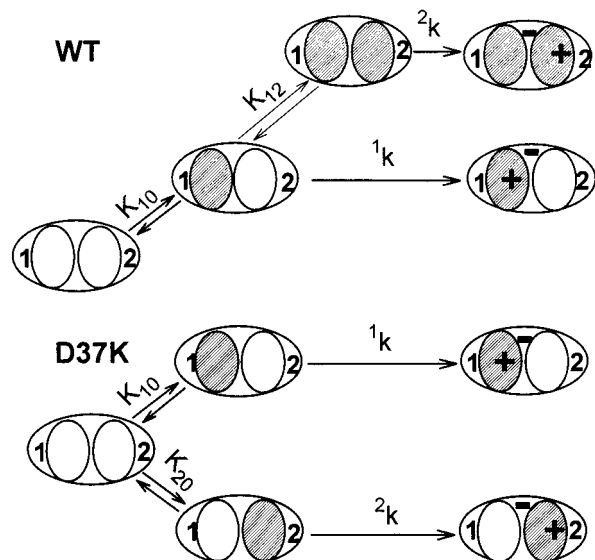


Figure 6. Schematic representation of dominant bindings and reaction pathways as described in the text. For CcP(WT), Cc almost exclusively follows the binding stage of the upper pathway, with essential none of [0,1] species formed. In contrast, for CcP(D37K), Cc binds at the two domains with comparable affinities.

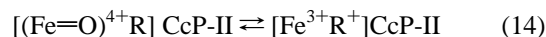
the dominant contribution to the quenching is from the 1:1 stoichiometry. As represented graphically in Figure 6, the first binding step occurs almost exclusively at domain 1 of CcP(WT) in the heme ET-inactive 1:1 complex [1,0] ($f_1 = K_{10}/K_1 > 98.5\%$; $^1k \leq 4.5$ s⁻¹).²⁰ Nonetheless, the reactivity is dominated by Cc bound at domain 2 in the highly reactive 1:1 complex [0,1] ($^2k > 2500$ s⁻¹).²⁰ For CcP(D37K), the mutation of Asp 37 to Lys 37 of CcP reduces K_{10} to the point that the two domains bind a Cc with comparable affinity. As a result, the first stoichiometric binding step occurs with only moderate affinity but now involves substantial formation of the highly reactive 1:1 complex [0,1], with $f_2 > 34\%$. In effect, the mutational weakening of the binding at domain 1 acts to *strengthen* binding to the highly reactive domain 2 by *ca.* 2 orders of magnitude. The result is described by eq 12: the stoichiometric rate constant k_1 is increased significantly, even though the domain rate constants are not affected by the mutation. Based on the estimate for the domain binding constant ($K_{20} \geq 4.3 \times 10^3$ M⁻¹), the upper limit for 2k can be set up as $^2k(\text{D37K}) < 4000K_1/(4.3 \times 10^3) \approx 1.2 \times 10^4$ s⁻¹.

The ionic strength dependence of k_1 for the ZnCc-Fe³⁺CcP(D37K) system likewise can be explained in terms of the relations between the stoichiometric and domain constants (eqs 9 and 12) if both K_{10} and K_{20} decrease as the ionic strength increases, with K_{10} decreasing more slowly. In this case, k_1 decreases from 3900 to 1000 s⁻¹ because the fraction of the heme ET-inactive 1:1 complex [1,0] increases as the ionic strength increases. K_{10} and K_{20} respectively incorporate the electrostatic interactions of the positively-charged, heme-exposed edge region on Cc with the negatively-charged domain 1 and domain 2 on CcP(D37K). Their ionic strength dependences could differ because the repulsive electrostatic interactions of the positively-charged residue Lys 37 at domain 1 of CcP(D37K) with the positively-charged lysine residues around the heme-exposed edge of Cc is weaker at higher ionic strength due to the charge screening effects.

Comparison with Studies That Involve Ruthenated Iron

Proteins. The definitive finding that direct heme-heme ET is more efficient in the 2:1 complex than in the 1:1 complex is coupled with strong evidence that the more tightly binding domain (1) exhibits poor heme-heme ET,^{32-36,38} whereas the domain with weaker binding (2) is highly reactive for direct heme-heme ET.²⁰ This suggests that direct ET to the Trp⁺ radical site occurs at the binding domain identified by the X-ray structure, which certainly must be associated with the kinetically detected domain 1, but that this domain may have lesser activity for direct heme-centered reactions. It has been argued that flash photolysis studies with ruthenium-labeled Ccs and ES^{32-36,38} rule out such a suggestion and, indeed, rule out two-domain reactivity. We now suggest that these studies instead fully support the two-domain picture.

The approach of covalently attaching a photoactive inorganic redox complex to a specific surface amino acid residue of a redox-active protein has revolutionized the study of *intraprotein* ET.¹² The extension of these methods to the study of inter-protein ET between redox centers in noncovalent protein-protein complexes has the potential advantage that it can be used to study any protein pair, including those in which *neither* partner contains a heme. However, the attachment of a large and often highly charged Ru complex can strongly perturb the delicate balance of interactions that govern complex formation, thereby having a profound effect on the strength and even the mode of protein-protein binding. Ignoring for now such issues, these studies^{32-36,38} indicate that Cc bound at the tight binding domain reduces the Trp radical, not the heme site, so that the product of the first such reduction of ES is CcP(h), in which the one oxidizing equivalent is on the heme. It is further suggested that this is followed by rapid intramolecular ET between the oxidized heme and the Trp to generate CcP(r) as the net product of the first reduction of ES by Fe²⁺Cc bound at domain 1 (eq 14). Return to the resting state, then, involves



reduction of the radical in CcP-II(r). In this process, ferryl-heme reduction is the result not of direct transfer to the heme but of a two-step process that involves the Trp. From this it is concluded that the heme-centered reduction and the Trp-centered reduction proceed along a common "pathway" and that both oxidizing equivalents *necessarily* are transferred to the Cc through a common binding domain. However, a number of considerations show this conclusion to be invalid. First, the reactions are carried out under highly nonphysiological conditions in which the concentration of Fe²⁺Cc is comparable to or less than that of ES. But these conditions assure that binding occurs only at the strong binding domain and preclude examination of the weak binding one! In other words, while the experiments elegantly demonstrate that heme reduction at domain 1 can generate CcP-II(h) in a two-stage process, from cytochrome to Trp to ferryl-heme, the experimental conditions in fact eliminate the possibility of detecting *direct* heme-heme ET from a cytochrome that binds and reacts at the second domain. Thus, the conclusion that heme reduction occurs only by reaction at domain 1 is rather a consequence of the measurement technique. One should also recall that intraprotein ET between heme and Trp is a (poorly understood) process that, under some circumstances, can be far slower than rates measured

for reduction by Cc.^{7,8,10} Most importantly, note that CcP-II(h) can be prepared as a *stable* species, with *no* evidence for the formation of CcP-II(r) species.

The two-domain binding model can also be applied to the recent study of a surface mutant reported by Miller et al.³⁴ In this study, the introduction of a bulky sulfhydryl group to CcP double mutant at position Cys 193 was used to weaken binding to the binding domain detected by X-ray diffraction, which the present work confirms to be associated with domain 1. Unfortunately, these authors did not provide any data for the binding affinity, and we cannot compare binding constants, presuming, of course, that values obtained in the presence of the perturbing Ru complex can be compared. As in the present case, they did not detect any 2:1 complex. In part this is because of the limitations in their experimental design noted above; in part it is because, as explained above, weakened binding to one of the domains necessarily decreases the stoichiometric constant, K_2 (eq 10). They also noted that the observed ET rate constant is changed after double mutation and attachment of a bulky group. They interpreted their observations in the context of two 1:1 complex conformers with Cc bound at two different sites within the broad, strong binding domain (H-mode and Y-mode). However, without any evidence to indicate that they could resolve a static unimolecular ET process involving a single conformer, it is unlikely that they have obtained site or domain constants, but rather only determined a stoichiometric rate constant, which is the sum of the weighted contributions from all possible 1:1 complex conformers with Cc bound at domains 1 and 2. Based on the reported data, they cannot rule out the existence of two distinct binding domains on CcP or the importance of contributions from a 1:1 complex with Cc bound at domain 2. Furthermore, the yCc dependence of steady-state activity of CcP(MI) at three different ionic strengths can be equally well interpreted by the model of two distinct binding domains on CcP. At $\mu = 20$ mM, the population of 1:1 complex with Cc at domain 1 [1,0] is much higher than that of 1:1 complex with Cc at domain 2 [0,1]. Since [1,0] is much less reactive than [0,1], the first saturation value of ν_0 , i.e., the y-intercept, is low, about 6 s^{-1} . When the ionic strength increases to 40 mM, the contribution of [0,1] is enhanced due to the differential dependence of domain binding constants K_{10} and K_{20} on ionic strength, leading to a value of 50 s^{-1} for the y-intercept. The further increase of ν_0 with yCc concentration after the first saturation is likely related to the contribution of 2:1 complex [1,1], whose formation follows 1:1 complex. At a high ionic strength of 100 mM, the binding affinity for 1:1 complex is much weaker, and the saturation of ν_0 is no longer as evident as it is at lower ionic strength. The y-intercept, therefore, is disappeared. But, the contribution of reactive [0,1] complex is even higher, and the value of k_{cat} is much higher. The change in the ionic strength dependence of k_{cat} is reflective of the variation of the contribution from complexes [0,1] and [1,1] and of different reactivities between [0,1] and [1,1].

The heme substitution titration procedures, in contrast, are successful in characterizing the two-domain binding and in demonstrating direct heme–heme reactivity at the more weakly binding domain, in part because metal substitution simplifies the reaction mechanism by observing only the heme–heme process. It is also in part because the quenching measurements more accurately mimic the physiological situation in which cytochrome *c* is in abundance, which, therefore, would facilitate the operation of *parallel* reaction processes (and pathways), in

one of which the CcP ferryl heme is directly reduced by a Cc bound at domain 2. In fact, the heme substitution measurements described above show that Cc bound at domain 1 does not undergo heme–heme ET when the Trp radical is not present but that this does *not* eliminate heme-centered ET to Fe^{2+}Cc , thereby disproving the notion that there is but one “portal” for the entry of reducing equivalents into CcP. Indeed, the rate constant for the reduction of ZnCcP^+ by Fe^{2+}Cc is quite similar to the rate constant reported for the heme-centered reduction of CcP-II,^{32–36,38} and thus, metal substitution *demonstrates* the presence of an ET pathway to the CcP heme that does not involve transient oxidation of Trp 191. The reasonable overall conclusions are that (i) reduction of the Trp radical occurs preferentially at domain 1; (ii) under conditions where equilibration of CcP(h) and CcP(r) is slow compared to the rapid heme reductions at domain 2, heme reduction might occur preferentially at this domain; (iii) whereas under conditions where equilibration is slow, heme reduction by Fe^{2+}Cc occurs independently at both domains, through a two-step process at domain 1 but directly at domain 2. One might surmise that misplaced emphasis on reactivity at a single domain in part may be inspired by inappropriate use of the X-ray structure of the 1:1 complex. Whereas crystallization selects the least soluble species from a solution, this need not correspond to the most active species, and it certainly need not be the only reactive one.

Summary. CcP binds Cc at two distinct binding domains, one having high affinity and the other having low affinity.^{11,18–21,29,30,45–52} Charge-reversal substitution of the negatively-charged residue Asp 37 of CcP by a positively-charged lysine strongly suppresses the 1:1 binding of Cc, thereby identifying residue 37 as part of the surface domain of CcP-(WT), denoted domain 1, that binds Cc with high affinity. This assignment also is consistent with domain 1 being the binding surface observed in the Cc–CcP crystal structure,⁵⁴ which shows the positively-charged Lys near the center of the interaction. The diminished ability of CcP(D37K) to bind Cc at domain 1 also suppresses binding of a second Cc molecule to form a ternary complex. However, the mutation sharply increases the observed reactivity of Cc. This happens because the mutation increases the *fraction* of the 1:1 complex where Cc is bound at the heme-reactive domain 2, i.e., $f_{20}(\text{D37K}) > f_{20}(\text{WT})$ (eq 12), which in turn causes CcP(D37K) to exhibit greater reactivity than CcP(WT). The results further demand that the two distinct binding domains on CcP are differentially affected by ionic strength. This overall picture is supported by a careful reconsideration of the most recent work from other laboratories.^{32–36,38} We hypothesize that domain 1, which the present results suggest closely corresponds to the crystallographic domain, may make the dominant contribution to the reduction of the Trp 191 radical, while domain 2, which is likely around the surface area including Asp 148 as predicted by the electrostatic calculation, provides the dominant kinetic site for ferryl–heme reduction. Further work on probing the weak binding domain (domain 2) is in progress.

Acknowledgment. We are grateful to Dr. Judith M. Nocek for helpful discussion. This research was supported by the National Institute of Health, Grants HL 13531 to B.M.H. and GM 21461 to G.M.

JA962399Q